A canstatin-derived peptide provides insight into the role of Capillary Morphogenesis Gene 2 in angiogenic regulation and matrix uptake

Jordan G. Finnell[a,‡], Tsz-Ming Tsang [a,‡], Lorna Cryan, Samuel Garrard[a], Sai-Lun Lee[a], P. Christine Ackroyd[a], Michael S. Rogers[b], Kenneth A. Christensen[a*]

[a]Department of Chemistry and Biochemistry, Brigham Young University, Provo, Utah, United States of America 84602. Email: J. Finnell, jfinnell@byu.edu; T. Tsang, ttming@byu.edu; S. Garrard, sam.garrard@byu.edu; S.L. Lee, leesailun91@gmail.com; P.C. Ackroyd, ackroyd@byu.edu

[b]Department of Surgery, Vascular Biology Program, Children's Hospital Boston, Harvard Medical School, Boston, Massachusetts, United States of America 02115. Email: M.S. Rogers, Michael.rogers@childrens.harvard.edu

*Corresponding author: kenc@chem.byu.edu

Abstract

Capillary Morphogenesis Gene 2 (CMG2) is a transmembrane, integrin-like receptor and the primary receptor for the anthrax toxin. In addition to its role as an anthrax toxin receptor, reports have repeatedly demonstrated that CMG2 plays a role in angiogenesis. Despite this, the molecular mechanism mediating observed CMG2-related angiogenic effects have never been fully elucidated. Previous studies have found that CMG2 binds type IV collagen (Col-IV), a key component of the vascular basement membrane, as well as other ECM proteins. Currently, no link has been made between these CMG2-ECM interactions and angiogenesis; however, ECM fragments are known to play a role in regulating angiogenesis. Here, we further characterize the CMG2-Col-IV interaction and explore the effect of this interaction in angiogenesis. Using a peptide array, we observed that CMG2 preferentially binds peptide fragments of the NC1 (non-collagenous domain 1) domains of Col-IV. These domains are also known as the fragments arresten (from the α1 chain) and canstatin (from the α2 chain) and have documented antiangiogenic properties. A second peptide array was performed to map a putative binding epitope. One top hit from the initial array, a canstatin-derived peptide, binds to the CMG2 ligand-binding von Willebrand factor A (vWA) domain with high affinity (peptide S16, $K_d = 400 \pm 200$ nM). This peptide competes with anthrax protective antigen (PA) for CMG2 binding, suggesting that, like PA, S16 interacts with CMG2 at the metal-ion dependent adhesion site (MIDAS) of its vWA domain. We demonstrate that CMG2 mediates endocytic uptake of S16, since CMG2-/- endothelial cells show markedly reduced S16 uptake, but no decrease in fluid-phase marker uptake. Furthermore, we show that S16 reduces endothelial migration but not cell proliferation. Together, our observations suggest that CMG2 may act as a receptor for Col-IV NC1 domain fragments, which provides an important mechanistic insight to the role of CMG2 in angiogenesis and extracellular matrix homeostasis.

Introduction

CMG2, also known as ANTXR2,[1] is an integrin-like receptor that was originally identified as a gene that is highly upregulated during endothelial cell tube formation *in vitro.*[1] Like integrins, CMG2 contains an extracellular vWA[1] domain that coordinates a divalent metal ion in a MIDAS[1] domain and binds various extracellular matrix proteins. The initial report qualitatively showed CMG2 binding to Col-IV,[1] fibronectin, and laminin;[1] subsequent reports indicate that CMG2 also binds Col VI.[2] However, the affinity, specific binding sites on each ECM, and the cellular relevance of these interactions have only been superficially examined.

CMG2, along with its close homolog TEM8, are most studied in their role as anthrax toxin receptors. These two cellular receptors bind the non-toxic anthrax toxin subunit, protective antigen (PA), and subsequently mediate intracellular delivery of the catalytic toxin subunits.[3, 4] Experiments that challenged mice lacking full-length CMG2 or TEM8 with *B. anthracis* spores indicate that CMG2 is the major receptor of anthrax toxin.[5] Biophysical characterization also demonstrates that PA has a substantially higher affinity (100 fold) for CMG2 than for TEM8.[6, 7]

While interaction of CMG2 with PA does not illµMinate the role of CMG2 in the absence of anthrax toxin, the tight interaction of CMG2 with PA has been used to probe the role of ligand interaction with CMG2 in angiogenesis. Notably, the binding of a mutant PA, (PA-SSSR) to CMG2 substantially inhibits angiogenesis in the cornea, reduces tµMor volµMe *in vivo,* and blocks endothelial cell migration *ex vivo.*[8] These data indicate that interaction of ligands with CMG2 has a profound effect on angiogenic

---

Abbreviations: CMG2, Capillary Morphogenesis Gene 2; MIDAS, metal ion dependent adhesion site; ECM, extracellular matrix; BM, basement membrane; VBM, vascular basement membrane; BLI, bio-layer interferometry; TEM8, TµMor Endothelial Marker 8; Col-IV, Type IV Collagen; Col-VI, Type VI Collagen; ANTXR2, Anthrax toxin receptor 2; vWA, von Willebrand factor type A;; PA, anthrax protective antigen; PA-SSSR, a furin protease resistant version of PA; HFS, hyaline fibromatosis syndromes; NC1, non-collagenous domain; CMG2-GST, a glutathione-s-transferase fusion with the vWA domain of CMG2;

processes. Further, knockdown of CMG2 in endothelial cells has been reported to inhibit their proliferation and tubule formation,[9] and several additional studies have demonstrated the relevance of CMG2 targeting in the inhibition of angiogenesis.[10-13]

Substantial data indicate that CMG2 is also important for extracellular matrix (ECM) homeostasis. Mutations in CMG2 that result in loss of CMG2 function are responsible for a severe genetic disorder known as HFS.[14-17] HFS is characterized by aberrant accμMulation of hyaline material under skin and in other organs. Recently, a publication by Bürgi et al. sheds light on the mechanism by which this might occur; wild-type CMG2 was found to mediate cellular uptake of type VI collagen (which accμMulates in HFS patient nodules), without affecting mRNA levels.[2]

There has previously been no functional connection between the role of CMG2 in ECM homeostasis and the role of CMG2 in angiogenic regulation. However, remodeling of the vascular basement membrane (VBM, composed predominantly of Col-IV, laminins, Col-VI, and other glycans) is an essential step in angiogenesis.[18] Hence, it is possible that CMG2 may regulate angiogenesis through VBM/ECM remodeling, which may occur in part via ECM uptake. This hypothesis is consistent with the observation that CMG2 endocytoses Col-VI and/or Col-VI fragments, and with buildup of Col-VI in HFS patients that lack functional CMG2.[2]

Individual ECM fragments themselves can have angiogenic impacts. Specifically, liberated Col-IV C-terminal NC1 domains have been well characterized as potently anti-angiogenic.[19-21] These domains appear to act in a negative feedback loop: as angiogenesis proceeds, the VBM is remodeled to allow vessel outgrowth, while at the same time newly-generated Col-IV NC1 fragments engage endothelial receptors to suppress further vessel sprouting. Importantly, Col-IV NC1 domains are essential for both proper triple-helix formation (through NC1 domain trimerization) and ECM network formation (through dimerization of adjacent NC1 trimers). While the 6 distinct Col-IV chains can trimerize in 3 different combinations,

the most abundant Col-IV isoform, including within the VBM, is composed of two α1 chains and an α2 chain. The NC1 domains of the α1 and α2 chains are arresten and canstatin, respectively.

Aspects of the mechanism(s) by which arresten and canstatin inhibit angiogenesis have been described, including identification of specific integrin receptors and downstream signaling pathways.[22-24] However, the ultimate fate of these Col-IV NC1 domains, including potential receptor-mediated endocytic and degradation pathways, has not been outlined. Given the established interaction between CMG2 and Col-IV, and the involvement of CMG2 in both ECM homeostasis and angiogenic processes,[1, 2, 9, 12] it is possible that these fragments are interacting with CMG2 and are taken into cells via interaction with CMG2. If so, this interaction could be in part responsible for the anti-angiogenic effects of CMG2 targeting. Hence, we undertook investigations designed to determine whether possible proteolytic peptide fragments of the NC1 domain could interact with cell-surface CMG2 and therefore influence angiogenesis.

Here, we report and characterize a novel interaction between CMG2 and peptide fragments of canstatin and arresten. This unanticipated interaction was initially observed via analysis of overlapping peptide arrays of Col-IV α1 and α2 sequences, which identified peptide sequences in the Col-IV NC1 domain as possible CMG2 binding sites. Peptide array hits with the highest intensity were synthesized for further binding analysis and characterization of their anti-angiogenic effects. Significantly, a canstatin-derived 15-mer peptide (denoted as S16) exhibited both high affinity for CMG2 and potent blocking of endothelial cell migration, suggesting that this small peptide can mimic the anti-angiogenic behavior of full-length NC1 domains. CMG2 mediates endocytosis and perinuclear-lysosomal delivery of this peptide fragment, consistent with a role for CMG2 in ECM/VBM fragment clearance. These findings suggest that CMG2 may play an important role in the regulation of angiogenesis by Col-IV NC1 fragments, and that

uptake and degradation of these antiangiogenic VBM fragments could be a potential functional explanation for the pro-angiogenic behavior of CMG2.

Materials and Methods

Protein preparation

HμMan CMG2 vWA-GST (CMG2-GST), CMG2 vWA R40c and C175A, and PA were expressed and purified as previously described[25]. Briefly, CMG2 vWA (40-217) was expressed with R40C and C175A mutations (R40C provides an exposed site for maleimide labeling; and C175A removes a buried cysteine to ensure a 1:1 labeling ratio) from a pGEX-4T1 vector. HμMan CMG2 -GST was expressed in BL21 T7 Express *E. coli* (New England Biolabs) with 0.5 mM IPTG induction in a 5L bioreactor (Sartorius). Cells were lysed via French press and sonication, and CMG2-GST was affinity purified with Glutathione Superflow Agarose (Thermo Fisher). Glutathione was removed and CMG2 exchanged into HBS-T with 50% glycerol using Sephadex G50 (GE Life Sciences) on an Äkta Start chromatography system.

PA-SSSR and PA-E733C were expressed from pET-22b (RRID: Addgene 11079) into the periplasm and purified from the periplasmic lysate via anion exchange chromatography (Q-sepharose, GE Life Sciences Cat: 25236), using 20 mM Tris-HCl pH 8.0 with 20 mM NaCl (Buffer A) and Buffer A + 1 M NaCl. Endotoxin was removed by passing twice through poly-lysine coated cellulose beads (Thermo Fisher Cat: 88275) followed by an endotoxin test using the gel clot method and appropriate dilutions.

CMG2-GST (AlexaFluor 488 or biotin) and PA-E733C (Alexa Fluo 546) were conjugated on a single reactive cysteine with maleimide-labels (Thermo Fisher) after GST was cleaved by using thrombin. Label:protein ratio was 5:1 in the reaction mixture. Conjugated protein was then purified from free label by size exclusion (Sephadex G50). All protein stocks were stored at -80°C in 50% glycerol.

Peptide S16 (PAIAIAVHSQDV) was synthesized (Genscript and Biomatik). Peptide U12 (VSIGYLLVKHSQTDQ) and scrambled S16 peptide (SPIAVDVQSAPIHAI) were synthesized (Genscript). S16 conjugated at the N-terminus to HiLite-488 was also synthesized (Anaspec).

Membrane-based peptide array with 10 residue sliding window

An overlapping peptide array (15 residue peptides, with a 5-residue overlap) containing the Col-IV α1 (Uniprot P02462) and α2 (Uniprot P08572) sequences was created by direct synthesis of peptides onto an amino-PEG cellulose membrane (ABIMED peptide array; Koch Institute Biopolymers and Proteomics Facility). The membrane was blocked in TBST with 1% milk, then probed with 250 nM CMG2-biotin. Bound CMG2-biotin was detected by avidin-HRP. Spot intensities were visually scored from 0 (no observed binding) to 5 (max binding).

PEPperPRINT peptide micro-array with 2-residue sliding window

A peptide array containing the Col-IV α1 and α2 NC1 domains (15 residue peptides with a 13-residue overlap) was printed by PEPperPRINT and probed according to manufacturer recommendations with 2 μM CMG2-GST then anti-GST- DyLight 800 4X PEG (RRID: AB_2537633). The raw TIFF image was analyzed by PepSlide® Analyzer (Sicasys).

From the quantified data and visual inspection, peptide hits flanked by adjacent hits are considered a potential binding surface. Hits with irregularly shaped noise or background were eliminated from further analysis. Epitope mapping molecular graphics were made in the PyMOL Molecular Graphics System, Version 2.0 Schrödinger, LLC.[26]

GibbsCluster-2.0[27, 28] was used to perform clustering analysis on array hits. Parameters were systematically varied in order to evaluate the effect of motif length and insertions and deletions on the quality of the alignment. A visual representation of these analyses was generated by Seq2Logo.[29]

CMG2-PA FRET assay

Interaction between CMG2 and peptides were measured using an *in vitro* FRET assay to detect competition with PA, as described previously.[13] Briefly, 10 nM each of CMG2-488 and PA-546 were incubated in the presence of peptide of varying concentration, with DMSO as vehicle control. FRET ratio = $I_{485/590}$ / $I_{458/528}$. FRET ratio with 10 mM EDTA was set to 0.

Bio-layer interferometry

Bio-layer interferometry was used to characterize the interaction of peptides with CMG2. Assay buffer was 50 mM HEPES, 150 mM NaCl, pH 7.2, 0.1% Tween-20, 1 mg/mL BSA, 2 mM $CaCl_2$, 1 mM $MgCl_2$, 0.02% NaN_3. First, streptavidin biosensors (ForteBio) were coated with 5-10 µg/mL CMG2-GST-biotin overnight at 4°C. Eight sensors were loaded and run in parallel (6 sensors for S16 binding, 2 for reference controls). Binding assays were performed the following day, using an Octet RED96 biolayer interferometer (ForteBio) and the Octet 8.2 Data Acquisition software. Assays were performed at 30°C and 1000 rpm shaking. The CMG2-GST-biotin loaded sensors were equilibrated in assay buffer (1200 sec) followed by an association step with a serial dilution (1-90 µM) of peptide (300-1200 sec), and a dissociation in assay buffer (600-1800 sec). Binding data for S16 concentrations below 1 µM were not obtainable, due to the low signal/noise ratio at sub-micromolar concentrations. Data was processed and analyzed in the Octet Data Analysis 8.2 software. Processed data was fit to a 1:1 binding model to obtain

kinetic and thermodynamic parameters. Residuals were examined to assess quality of fit and no systematic deviation was observed.

Cell lines and culturing technique

EOMA (CRL-2586, RRID:CVCL_3507) is a murine hemangioma endothelial cell line.[30] EA.hy926 (CRL-2922, RRID:CVCL_3901) cells are the result of a fusion of hµMan µMbilical vein cells with lung carcinoma cells[31]. Both cell lines were cultured in 10% FBS + DMEM and incubated at 37ºC in a hµMidified environment with 5% CO_2 until ready for passaging.

Endothelial cell binding assays by flow cytometry

Cells were cultured in well-plates to 30-70% confluence. Cells were incubated in 10% FBS DMEM and treated with 200 nM PA-SSSR when indicated. Cells were co-treated with S16-Alexa Fluor 488 conjugate (2 µM), transferrin-Alexa Fluor 633 conjugate (10 µg/mL ThermoFisher, Cat: T23362), or Dextran 10,000 MW Texas Red (100µM ThermoFisher, Cat: D1863), and incubated at 37°C for indicated times. When indicated, a well plate with staining media supplemented with 20mM HEPES was left on ice for the indicated time. After incubation, cells were washed, trypsinized, and spun down, then resuspended in cytometry buffer (PBS, 1% BSA, 5 mM glucose) and analyzed in an Attune Acoustic Focusing Cytometer, equipped with 488nm and 633nm lasers. Experiment that used Dextran-Texas Red was analyzed with Cytoflex Cytometer, equipped with 401nm, 488nm, 561nm, and 638nm lasers. Cytometry data was analyzed in FlowJo.

Confocal microscopy to track ligand endocytosis

Cell preparation and staining for confocal microscopy was as described above for flow cytometry, except that cells were seeded in appropriate glass bottom culture dishes. Staining with S16-488 (2 μM) and transferrin-633 (10 μg/mL) was performed at 37°C for 1-3 h, washed three times with serμM-free media, then incubated with a low fluorescence media supplemented with ProLong live-cell antifade reagent (ThermoFisher Cat: P36975) at 37°C for at least 1 hour. Live-cell images were acquired on a Leica DMi8 confocal microscope, using 488nm and 633nm lasers. Images were acquired with the Leica Application Suite X (LAS X), deconvoluted in Huygens Essential, and further analyzed in LAS X to examine colocalization.

Wound-scratch migration assay

EOMA cells were seeded in 96 well plate and cultured in 10% FBS DMEM. Cells were incubated at 37°C in a hμMidified environment with 5% CO_2 until completely confluent. A 200 μL pipette tip was used to scratch a wound in the monolayer, followed by three washes with PBS. Cells were then treated with 10% FBS DMEM with or without S16, and serμM free DMEM as negative control. Images were acquired every four hours, and the change in wound area was quantified using ImageJ.

Cell proliferation assay

15,000 EOMA cells were seeded into each well in a 96 well plate and incubated for 1 h to attach. After cell attachment, media with treatments were added. Ethanol-fixed cells were used as negative control. After a 24 h incubation, 20 μL CellTiter-Blue Reagent (Promega Cat: G8080) was added to each well for 4 h. Fluorescence signal (Ex: 560nm / Em: 590nm) was measured using a BioTek Synergy H2 plate reader. All readings were normalized to the non-treated control.

CellAsic migration assay

The assay protocol followed the CellASIC ONIX M04G-02 Microfluidic Gradient Plate User Guide. All media put into the plate (except the cell suspension) was filtered through a 0.2 µm syringe filter. EA.hy926 cells (3 x 10^6 cells/mL) were loaded in and incubated overnight with DMEM + 10% FBS under flow at 37ºC. Assays were then performed with a stable gradient of DMEM + 0 – 10% FBS with or without peptide treatment. Brightfield images at 10x magnification were taken every 10 min over 12 h on an Olympus IX73 microscope and the ORCA-Flash 4.0 camera (Hamamatsu). Individual cells were tracked with ImageJ (RRID: SCR003070) manual tracking plugin. Data was transferred to the ibidi Chemotaxis and Migration Tools 2.0 to export endpoint 'y' displacement and accµMulated displacement. P-values were calculated using Student's *t*-test and error bars are standard error of the mean (n=40).

Results and Discussion

CMG2 binds preferentially to the anti-angiogenic Col-IV NC1 domains

CMG2 has emerged as an important regulator of angiogenesis,[8, 9, 12] but there is still little insight into its mechanism. Given reports that CMG2 binds Col-IV[1] and that the Col-IV fragments arresten and canstatin have anti-angiogenic properties,[19-21] we investigated the putative interaction of the CMG2 vWA domain with Col-IV peptide sequences to shed light on the possible relevance of this interaction for angiogenic regulation. To identify peptide sequences on Col-IV that could be interacting with CMG2, we constructed a scouting peptide array in which the linear sequences of hµMan Col-IV α1 and α2 chains were directly synthesized onto a nitrocellulose membrane. The array consisted of 15-mer peptide units, with a 10-residue shift between subsequent peptides, and scanned the entire length of the α1 and α2 chains of Col-IV. The array was probed for CMG2 interaction with 250 nM CMG2-biotin and read out with avidin-HRP; spots representing binding of CMG2 to individual peptide sequences were visually scored

with intensities assigned from 0 (min) to 5 (max) (Fig 1a-b, Supplementary Fig 1). When these intensity values were plotted against the complete sequential protein sequence in the Col-IV α1 and α2 chains, we could visualize relative binding in different sections of the sequence (Figure 1a-b). For each chain, we observed sparse and weak CMG2 binding throughout the Col-IV 7S and triple-helical regions, but heavily concentrated binding within the Col-IV NC1 domains (Fig 1, Table 1). We quantified this binding by calculating a hit ratio and weighted hit ratio for each domain, calculated by adding the nμMber of hits or sμM of intensity scores in each domain, respectively, and dividing by the nμMber of peptides in that domain. This metric represents an average relative binding response for each domain. When the peptide array binding data were evaluated this way, we observed that arresten and canstatin exhibited much higher hit ratios (14-fold and 3-fold, respectively) and weighted hit ratios (25-fold and 6-fold, respectively) than their corresponding triple-helical or 7S domains (Table 1). This indicated that CMG2 was preferentially binding to NC1 domain-derived sequences on the peptide array, suggesting that CMG2 might primarily bind to a site or sites on the Col-IV NC1 domain.

We sought to further characterize the CMG2-NC1 interaction by mapping possible binding site(s) on the NC1 domain. While the initial peptide array strongly indicated that CMG2 binding is enriched in canstatin and arresten versus the rest of the Col-IV chains, the large sliding window for different peptides in this array made identification of the individual CMG2-binding residues within each peptide hit difficult. To identify the individual peptides in the NC1 domain that could be binding CMG2, we synthesized an additional peptide array on a glass chip, with the NC1 domains arrayed as 15-mer peptides in a 2-residue sliding window (Supplementary Figure 2). The goal was to use hits from overlapping peptides confirm the identity and sequence of CMG2-binding peptide regions in the NC1 domain. We defined a putative peptide hit as 3 or more consecutive peptides that showing binding to CMG2, and mapped identified CMG2-binding sequences onto a previously solved structure of the Col-IV NC1 domain hexamer (Fig 1c,

PDB: 1LI1)[32]. Notably, both canstatin and arresten fragment peptides identified as putative CMG2 interactors are localized on the accessible surface of the NC1 domain (Figure 1c, left), and therefore could be recognized by CMG2 for interaction in whole NC1 domain. Peptide fragments from arresten were also identified on the solvent-exposed surface (Fig 1c, right) although the CMG2-binding surface of arresten was sparser than for canstatin. Importantly, identification of individual CMG2 binding peptide fragments of arresten and canstatin, combined with their localization on the solvent accessible surface of the NC1 domain suggests the possibility that the antiangiogenic activity of arresten and canstatin could be regulated in part by interaction with CMG2.

CMG2 has high structural homology to many integrins,[6] whose ligands commonly have an established RGD motif.[33] Hence, we evaluated the 2-residue sliding window peptide array data to identify a possible consistent CMG2-interacting motif. Alignment of all hits from this array produced a consistent binding element distinct from the RGD motif of integrins that contained an aliphatic residue at the nth position, followed by an acidic residue at the $(n+2)^{th}$ position (Supplementary Figure 3). This observation is not entirely unexpected, as CMG2 ligands would be expected to have D/E residues that could participate in binding the divalent cation in the CMG2 MIDAS domain.[34] The binding motif identified in the evaluation of Col IV binding was not seen in Col VI, laminin, and fibronectin as determined by an NCBI protein BLAST alignment of the sequence.

Canstatin-derived peptide S16 binds with high affinity to CMG2 via the MIDAS

To further understand the relevance of CMG2 interaction with NC1-derived peptides, we further evaluated the top NC1 hits from the initial peptide array for CMG2 binding. Peptides from the NC1 region showing the maximμM binding score of 5 were selected; this yielded two peptides, denoted here as S16 and U12, both from canstatin. We synthesized these two peptides and characterized their interaction with

CMG2 using two *in vitro* assays: 1) a PA-CMG2 competition FRET assay,[13] and 2) a bio-layer interferometry (BLI) kinetic binding assay. These data show that both peptides U12 and S16 bind CMG2 and compete with PA for binding to CMG2. Peptide U12 showed relatively modest affinity for CMG2, both by BLI (K_d = 80 μM) and the FRET competition assay with PA (IC_{50} = 35 μM; Supplementary Figure 4). Peptide S16 bound CMG2 with much higher affinity. Analysis by BLI revealed that S16 binds CMG2 with sub-micromolar affinity: K_d = 0.4 ± 0.2 μM (Fig 2b, mean ± SD, n = 3 independent experiments). This interaction was characterized by a relatively slow on-rate (≈ 2×10^2 $M^{-1}s^{-1}$) and off-rate (≈ 1×10^{-4} s^{-1}). Further discussion on the observed kinetics is provided in Supplementary Note 1. Binding of CMG2 by S16 was corroborated by FRET competition with PA, in which the S16 IC_{50} was 2.7 μM (Fig 2a, 95% CI: 1.9-3.7) An estimate of the CMG2-S16 K_d obtained from the FRET competition IC50 data yielded a likely K_d of 100 ± 55 nM, in rough agreement with that measured by BLI.

To confirm specificity of CMG2 for S16, we synthesized a scrambled S16 peptide comprised of the same residues as S16 but in a random order and probed for interaction of this peptide with CMG2 via BLI. Unlike S16, this scrambled version of S16 peptide showed minimal binding of CMG2, even at concentrations up to 30 μM (Supplementary Figure 5). Additionally, the scrambled S16 binding data fit poorly to all available binding models tested (1:1, 1:2, and 2:1 bivalent models). These studies indicated that the S16-CMG2 interaction is sequence specific.

The ability of S16 to compete with PA for CMG2 binding, as identified in the FRET competition assay, suggests that S16 interacts with the ligand binding surface of the CMG2 vWA domain at the MIDAS, as does PA. BLI experiments were used to verify that S16 binds in competition with PA. Specifically, saturating CMG2-loaded biosensors with PA prior to exposure to S16 significantly reduced CMG2 binding to S16 (Fig 2c). As further support of MIDAS interaction, EDTA prevents S16 binding to

CMG2 (Fig 2d), confirming that the interaction is metal ion (Ca^{2+} or Mg^{2+}) dependent. Indeed, S16 contains an aspartate (preceded by several aliphatic residues) that could participate in metal coordination.

As described above, multiple independent assays demonstrate interaction of peptide S16 with the CMG2 vWA domain. Together, data from these assays demonstrate that this canstatin-derived peptide interacts with the CMG2 MIDAS, in a manner competitive with anthrax toxin PA, and with an affinity of ~0.4 μM. Considering the established role of CMG2 in angiogenesis and the anti-angiogenic activity of anthrax toxin PA[8] and the Col-IV NC1 canstatin[19], we asked whether this small fragment of canstatin (S16) can inhibit angiogenic processes in endothelial cells.

Peptide S16 inhibits endothelial cell migration, but not proliferation

Proliferation and chemotactic migration of endothelial cells are essential to angiogenesis. Previous work has shown that binding of angiogenesis-inhibiting molecules to CMG2, including PA and small molecules, inhibits migration but not proliferation of microvascular endothelial cells.[8, 10, 35] We first examined the impact of S16 on both proliferation and migration of EOMA cells. Like PA, S16 did not impact endothelial cell proliferation in EOMA cells (Fig 3a). However, in a standard wound scratch assay with EOMA cells, S16 exhibited strong inhibition of endothelial cell migration compared with the untreated, full-serμM control (Fig 3b). Indeed, there was no statistical difference in migration of S16-treated cells and cells without serμM, indicating that S16 completely blocked serμM-stimulated EOMA cell migration. S16 competes with PA for CMG2 binding, and PA is known to inhibit cell migration and other angiogenic processes.[8] Hence, the observation that S16 also inhibits migration suggests that the S16 exerts its angiogenic impact via interaction with CMG2.

The wound scratch assay is standard in assessing cell migration, but has notable drawbacks, including limited reproducibility and an inability to distinguish chemotaxis from chemokinesis. To

validate the anti-migration effects of S16 in an orthogonal migration assay, we investigated the impact of S16 in a microfluidic, chemoattractant gradient migration assay that utilized the CellASIC Onix microfluidic migration platform. This platform allows cells to migrate within a stable, unidimensional chemoattractant gradient that mimics the growth factor gradients present during physiological angiogenesis. In addition, this assay allows the movement of individual cells to be monitored over time, so that it is possible to distinguish between total cell movement (chemokinesis) and movement in the direction of the growth factor gradient (chemotaxis). Real-time tracking of EA.hy926 cells demonstrated strong chemotactic migration towards serμM (Fig 3c, e) in the absence of S16. In contrast, when cells were treated with S16, the observed movement of cells was a random walk (p=0.9 in Rayleigh test of circular uniformity) that ignored the chemoattractant gradient (Fig 3d-e). When compared to an untreated control, cell chemotaxis was nearly complete abolished (90%) by S16 treatment (as seen from cμMulative distance and 'y' distance migrated, Fig 3f), while chemokinesis exhibited only a modest reduction (20%). This near-complete abolition of chemotactic migration by S16 was consistent with near-complete lack of cell migration in the wound scratch assay. This specificity of S16 for inhibition of chemotaxis rather than bulk cell motion provides potentially important insights into the mechanistic function of CMG2 in endothelial cell migration and angiogenesis, especially in mediating endothelial cell chemotaxis. To confirm that the loss of chemotaxis results specifically from S16 peptide treatment, we repeated the CellASIC migration assay using the same scrambled peptide generated as a CMG2-binding control. Treatment with the scrambled peptide control showed no difference in either chemotaxis or chemokinesis between treated cells and vehicle (Supplementary Figure 6), demonstrating that the observed anti-migratory effect depends specifically on the amino acid sequence of S16.

CMG2 is the relevant endothelial surface receptor for S16 and mediates endocytosis of S16

Having determined that S16 binds to CMG2 with high specificity and affinity (Fig 2), and that S16 inhibits endothelial cell migration, we sought to confirm that CMG2 acts as an endothelial cell surface receptor for S16. Since we had already established that PA can compete with S16 for CMG2 binding, we compared the ability of S16 to bind the surface of EA.hy926 endothelial cells and be internalized in the presence and absence of 200 nM PA-SSSR. We chose PA-SSSR for this assay rather than PA-WT due to the previous observation that PA-SSSR has a more potent anti-angiogenic effects than PA-WT.[8] Using an N-terminal fluorescently labeled version of S16 (S16-488), we quantified cell binding of S16 by flow cytometry. We note that since these experiments quantify total cellular fluorescence, they do not distinguish between S16 fluorescence at the cell surface and intracellular fluorescence resulting from S16 endocytosis following receptor-binding. As shown in Figure 4a, S16-488 showed a time-dependent interaction with EA.hy926 cells that was drastically reduced (~ 60%) by co-incubation with PA-SSSR at concentrations high enough to compete any bound S16 off the cell-surface CMG2 (PA=200 nM) . In contrast, binding of a control cell-surface ligand, Transferrin-633, was unaffected by the presence of PA-SSSR (Fig 4b). These data indicate that S16 and PA-SSSR share a cell-surface receptor. Hence, the predominant S16 receptor is likely to be an anthrax toxin receptor that also binds PA. However, these experiments were carried out at 200 nM PA concentrations, which would be expected to substantially occupy both CMG2 and TEM8, and they do not clearly establish that CMG2 is the receptor which responsible for binding S16 at the cell-surface.

To evaluate if CMG2, rather than TEM8, is the receptor that interacts with S16 on the surface of endothelial cells, we compared binding of S16-488 to EA.hy926 WT and CMG2-depleted (CMG2-/-) cells. These data (Figure 4c) indicate that CMG2-/- cells display significantly less S16-488 signal than WT EA.hy926 cells (50%; $p<0.05$). This reduction is statistically identical to the reduction in S16-488 fluorescence observed in the presence of CMG2-saturating PA-SSSR concentrations (40%) indicating that

the reduction observed in the presence of PA-SSSR is due to CMG2 activity. Hence, S16 is interacting with CMG2, rather than TEM8, at the cell surface, consistent with our observation of CMG2-S16 binding *in vitro* (Fig 2). This conclusion that this Col-IV peptide fragment interacts with CMG2 rather than TEM8 at the cell surface is perhaps not surprising; while CMG2 has been identified as a receptor for Col-IV,[1] there is no evidence for interaction of Col-IV with TEM8.[36, 37]

Notably, experimental design for the cell-binding assay above involved harvesting of adhered cells with trypsin, which was likely to remove any extracellular S16 prior to flow cytometry analysis. Hence, the signal observed in the cell-binding experiments above was likely to reflect the presence of intracellular S16-488 taken into the cells via CMG2-mediated endocytosis, rather than S16 bound to CMG2 that remained on the cell-surface. To establish that surface-bound S16 was taken into cells by endocytosis, we compared S16-488 and Tf-633 fluorescence in EA.hy926 cells at 37°C to that of cells treated on ice, a condition that inhibits endocytosis.[38] The robust S16-488 and Tf-633 flow cytometry signal exhibited at 37°C was completely eliminated by incubation on ice (Fig 4d). Hence, observed signal reflected internalization via an endocytic mechanism. To confirm this finding and clarify whether S16-488 enters cells via endocytosis vs. fluid-phase pinocytosis, we used confocal microscopy to visualize the cellular uptake of S16-488 and Tf-633. We observed clear punctate intracellular colocalization of both ligands (Fig 4d, Supplementary Movie 1), with apparent vesicles visible throughout the cell, and concentrated around the nucleus in what are likely perinuclear lysosomes. Tf-633 is known to be taken into cells via receptor-mediated endocytosis and the presence of S16-488 in the same vesicular structures as Tf-633 indicates that S16-488 is taken into cells via the same process.

We note that both the CMG2-/- and PA-treated endothelial cells show a relatively high background of nonspecific uptake (40-50%). Constitutive fluid phase uptake will result in some level of S16 entry into the cell. Since CMG2 cell-surface expression in endothelial cells is low (CMG2 in Ea.hy926 cells could

not be detected by Western blot, but mRNA was detected by RT-PCR), the relative contribution of nonspecific fluid phase uptake to CMG2-mediated uptake is expected to be significant. Hence, the presence of intracellular S16 in the absence of CMG2 or in the presence of suturing PA-SSSR conditions (40-50%) reflects expected non-specific fluid-phase uptake that occurs coincident with CMG2-mediated S16 uptake. To verify that fluid phase uptake, or pinocytosis, can happen independent from CMG2 mediated endocytosis, we incubated EA.hy926 WT and CMG2-/- cells with a dextran Texas Red conjugate (internalized via fluid-phase uptake that does not involve receptor binding) and compared the dextran signal between the two cell lines. The resulting data showed that pinocytosis was still an ongoing event even after CMG2 was depleted from cell surface, consistent with some level of non-specific uptake of S16 (Supplementary Figure 7). Combining data from experiments above, we conclude that S16 can potentially be internalized via both non-specific pinocytosis and receptor-mediated uptake. This finding demonstrates a new role of CMG2 as a cell surface receptor that mediates the uptake of a Col-IV-derived peptide.

Together, the data presented in this work shows that a small peptide-segment of the anti-angiogenic Col-IV fragment canstatin (α2 NC1) binds to CMG2 with sub-micromolar affinity, via the MIDAS (Fig 2). The near-complete inhibition of endothelial cell chemotactic migration by this peptide that is demonstrated in two orthogonal assays (Fig 3), echoes the effect of other CMG2 antagonists[8, 10, 13, 35] and confirms a critical role for CMG2 in the cell migration required for angiogenesis.

Endothelial cells participate in ECM remodeling during angiogenesis, including inducing proteolytical cleavage of ECM materials that results in release of ECM peptides, which are then available for binding and/or endocytosis by cell-surface receptors. If CMG2 is involved in ECM homeostasis, as has previously been proposed,[2, 15-17] CMG2 could be one of the possible receptors that interact with such ECM peptides/fragments. Our flow cytometry and confocal microscopy data show that CMG2 both binds

and mediates internalization of peptide S16. This observation is supports a role for CMG2 in endocytosing ECM material, consistent with a previous report indicating that CMG2 is involved in uptake of ECM fragments.[2] CMG2-mediated endocytosis of a CMG2-binding molecule is also consistent with the established role of CMG2 in mediating clathrin-dependent endocytosis of the anthrax toxin.[2,39] It remains to be seen whether uptake of ECM/VBM-derived molecules, including peptide fragments, utilizes the same mechanism as endocytosis of anthrax toxin.[39-42]

Together, these findings suggest that CMG2 could act as a receptor for Col-IV NC1 fragments (Fig 1), including S16, and mediate the endocytosis that results in their eventual lysosomal degradation. This process provides one potential functional explanation for the pro-angiogenic behavior of CMG2. CMG2 interaction with, and endocytosis of, anti-angiogenic peptide fragments and/or protein domains such as arrestin and canstatin is expected to reduce their relevant circulating concentrations, and thus, their anti-angiogenic impact. CMG2 inhibitors such as PA, S16, and identified small molecules[10, 35] may thus inhibit CMG2-mediated arrestin or canstatin endocytosis and therefore magnify the anti-angiogenic impacts of these fragments. More work is needed to examine the mechanistic function of CMG2 in cell migration and to identify additional molecules involved in this process, which could be additional therapeutic targets for modulation of angiogenesis.

Acknowledgement

The plasmid pGEX4T1-CMG2-GST was a generous gift from the John Collier lab.

Tables

	# Hits (Total # Peptides)	Hit Ratio	Weighted Hit Ratio	Mean Spot Intensity± SEM ‡	# Hits (Total # Peptides)	Hit Ratio	Weighted Hit Ratio	Mean Spot Intensity± SEM ‡‡
7S	0 (14)	0	0	0 ± 0	1 (16)	0.063	1.56	0.3 ± 0.3
Triple-helical	5 (127)	0.039	0.551	0.05 ± 0.03	16 (129)	0.124	2.64	0.26 ± 0.07
NC1	13 (23)	0.565	13.9	1.5 ± 0.3	10 (24)	0.417	15.0	1.5 ± 0.4

‡ Tukeys post-hoc – 7S vs Triple-helical: $p = 0.9394$, NC1 vs 7S: $p < 0.0001$, NC1 vs Triple-helical: $p < 0.0001$
‡‡ Tukeys post-hoc – 7S vs Triple-helical: $p = 0.9827$, NC1 vs 7S: $p = 0.0009$, NC1 vs Triple-helical: $p < 0.0001$

Table 1. Binding profile quantification for CMG2 interaction with Col-IV-derived peptides. Hit ratio was calculated as # hits (intensity > 0) divided by total nµMber peptides in domain. Weighted hit ratio was calculated as total measured intensity of domain divided by total nµMber peptides in domain.

1 **Figures**

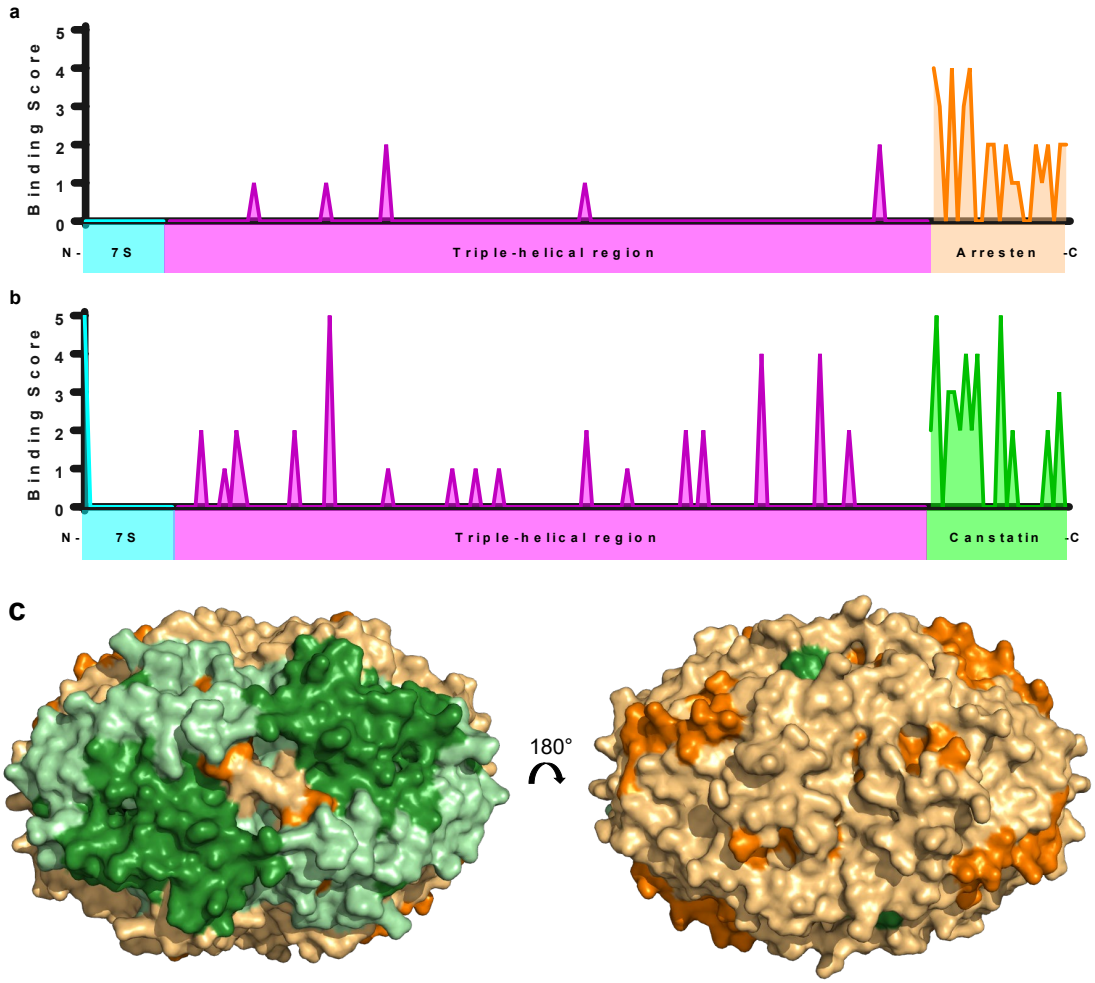

Figure 1. Peptide arrays identify CMG2 as a receptor of Col-IV NC1 domains. (a-b) A peptide array of 15-mer peptides with a 10-residue sliding window, covering the sequences of Col4A1 (a) and Col4A2 (b). This array was probed with 250 nM CMG2-biotin and read out using avidin-HRP. Spot intensities were scored from 0 (no observed binding) to 5 (maximal binding). Domain topology is shown below. There is a greater proportion of CMG2-binding peptides within the c-terminal NC1 domains than the collagenous and 7S domains. (c) PEPperPRINT peptide array with a 2-residue sliding window identifies a putative CMG2-binding surface. NC1 hexamer shown (PDB 1LI1) consists of two trimers, each composed of two arresten and one canstatin. Arresten is shown in orange; canstatin in green. Binding sequences are shown in darker shades. Left shows canstatin-exposed face, demonstrating a large, uniform epitope for CMG2 to canstatin. Right displays arresten-exposed face, where CMG2-binding peptides are present, but are more sparse.

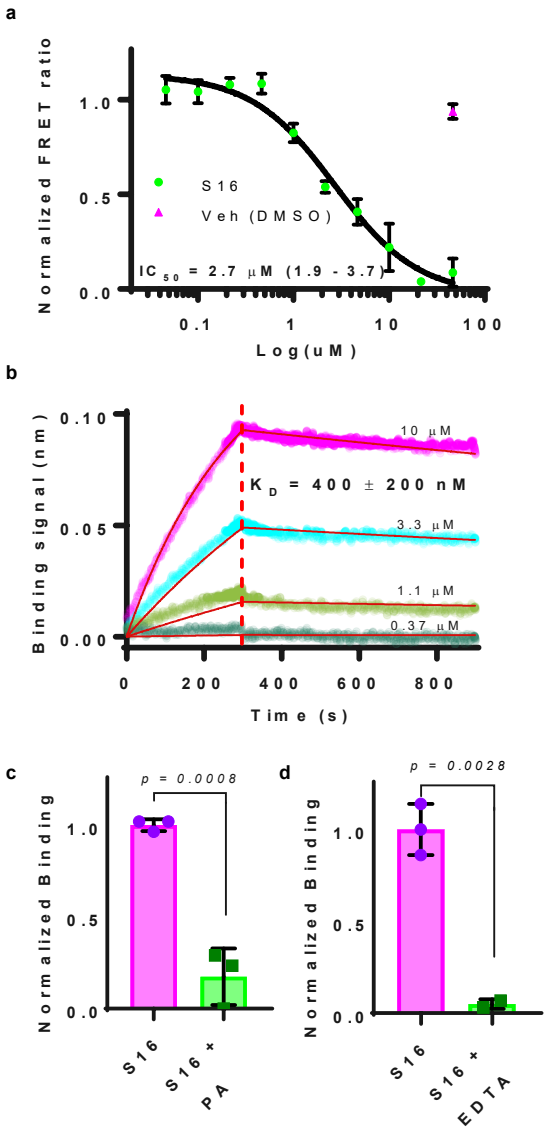

Figure 2. ***Peptide S16 binds to the CMG2 MIDAS with sub-micromolar affinity.*** (a) CMG2-488/PA-546 FRET inhibition assay confirms the specificity of S16 binding to CMG2. IC50 shown with 95% CI. (b) Representative experiment of S16 (concentration indicated) binding to CMG2-GST-biotin loaded BLI sensors. K_d shown is mean ± std (3 independent experiments). (c-d) Peptide S16 interacts with the MIDAS domain of CMG2. (c) CMG2-GST-biotin loaded BLI sensors equilibrated in buffer with or without 500 nM PA, followed by incubation in 10 µM S16 (n=3 per condition). (d) CMG2-GST-biotin loaded BLI sensors were equilibrated either in buffer with 2 mM $CaCl_2$ and 1 mM $MgCl_2$, or 10 mM EDTA, followed by incubation with 10 µM S16 (n=3 per condition). Error bars are standard deviation of replicates.

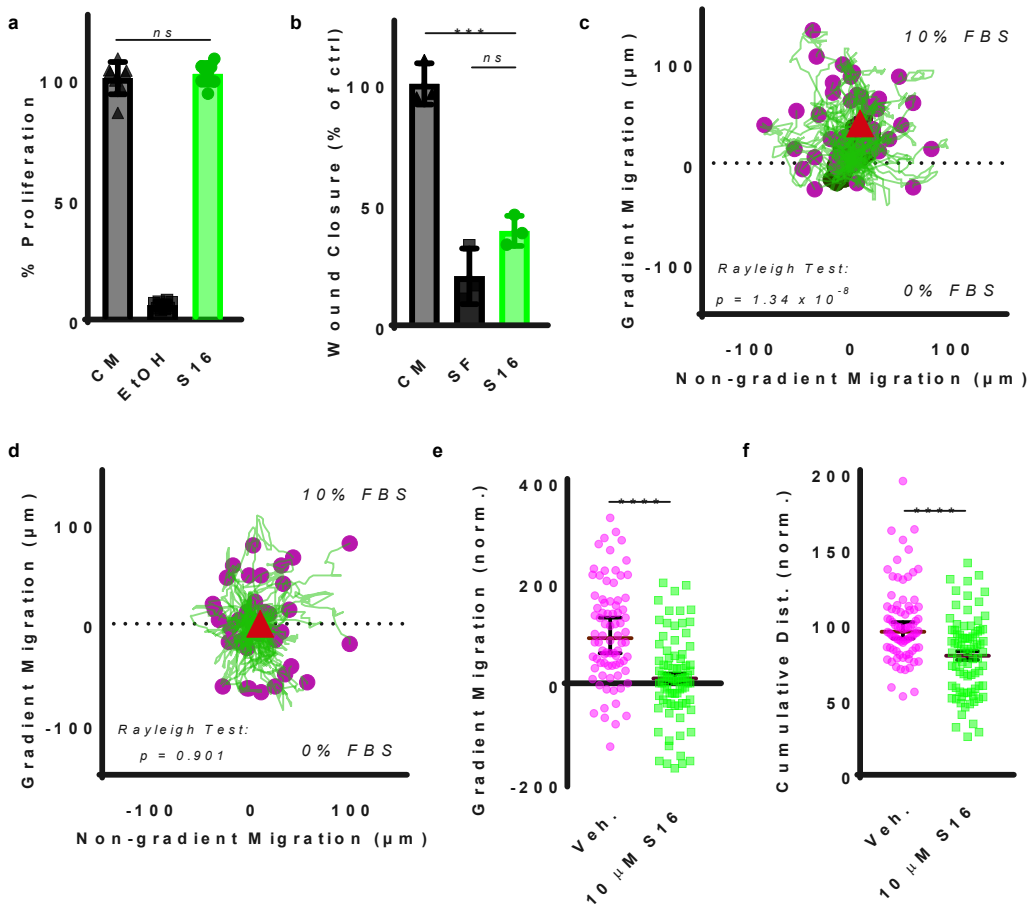

Figure 3. Peptide S16 abolishes migration of endothelial cells, with no effect on proliferation. (a) Proliferation of EOMA cells was monitored. Treatment with S16 resulted in no change in proliferation relative to the untreated control. In contrast, cells fixed in ethanol showed a complete loss of proliferation. Error bars are SD of n=7 replicates from two independent experiments. (b) Wound scratch migration assay. S16 results in 60% reduction in wound closure and is not statistically distinguishable from the serµM-free (negative) control. Error bars are SD of n=3 replicates. (c-f) CellAsic Chemotactic Migration assay with EA.hy926 cells. Individual cell tracks show cells migrating towards serµM in the control (c), but a complete loss in chemotactic migration with S16 treatment (d). "Center-of-mass" indicated by red triangle, shows net movement. Rayleigh p-value tests for deviation from circular uniformity. Comparative data for chemotactic migration (e) and cµMulative distance migrated (f) are shown. Error bars are SEM of n=50 cells for each condition. ***, $p < 0.001$; ****, $p < 0.0001$; ns, not significant.

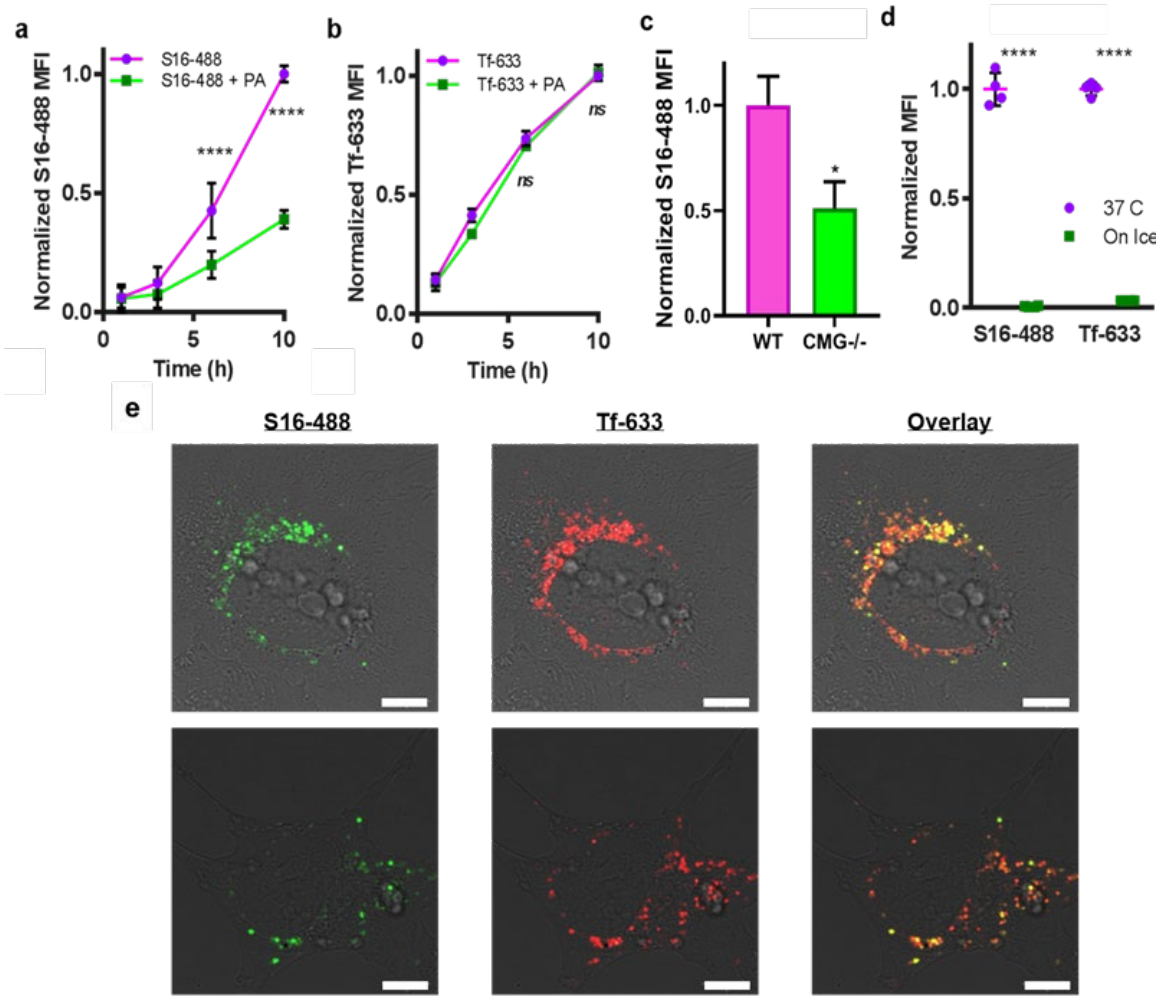

Figure 4: CMG2 is the relevant cell surface receptor for S16 and mediates S16 internalization (a-b) Flow cytometry analysis on timecourse of conditioned EA.hy926 cells treated with S16-488 (a) and transferrin-633 (b) with or without 200 nM PA-SSSR. Treatment with PA-SSSR specifically reduces binding of S16-488 to endothelial cells but does not reduce the binding of transferrin-633, demonstrating that at least 60% of S16 cell binding occurs through the anthrax toxin receptors. MFI, mean fluorescence intensity. N=6 from two independent experiments. (c) Flow cytometry analysis on EA.hy926 WT and CMG2-/- cells treated with S16-488. Depletion of CMG2 significantly reduced S16 binding to S16 in a similar manner as CMG2 inhibition by PA-SSSR. (d) Cold treatment abolishes the signal of both S16-488 and transferrin-633, indicating that, as transferrin, S16 is being internalized. Conditioned EA.hy926 cells were incubated with 2 µM S16-488 and 10 ug/mL transferrin-633 in DMEM (with 20 mM HEPES and 1% FBS) for 6 hrs, either at 37C or on ice. Cells were harvested and analyzed by flow cytometry. Plot shows mean fluorescence intensity of four replicates. (e) Conditioned EA.hy926 were incubated with 2 µM S16-488 and 10 ug/mL Tf-633 at 37C for 3 hours, then incubated in imaging buffer (SDM79 with 7.5 mM glucose and ProLong™ antifade) for 1 hr at 37C, then imaged by confocal microscopy. Representative images of two individual cell (top and bottom) are shown. Scale bar is 10 µM. Consistent colocalization between S16 and Tf in endosomes and in apparent perinuclear lysosomes was observed.

These findings were consistent across n=20 cells from 2 independent experiments; in every cell, endosomal and lysosomal colocalization was also observed. ****, $p < 0.0001$; ns, not significant.

References

[1] Bell, S. E., Mavila, A., Salazar, R., Bayless, K. J., Kanagala, S., Maxwell, S. A., and Davis, G. E. (2001) Differential gene expression during capillary morphogenesis in 3D collagen matrices: regulated expression of genes involved in basement membrane matrix assembly, cell cycle progression, cellular differentiation and G-protein signaling, *J Cell Sci 114*, 2755-2773.

[2] Burgi, J., Kunz, B., Abrami, L., Deuquet, J., Piersigilli, A., Scholl-Burgi, S., Lausch, E., Unger, S., Superti-Furga, A., Bonaldo, P., and van der Goot, F. G. (2017) CMG2/ANTXR2 regulates extracellular collagen VI which accµMulates in hyaline fibromatosis syndrome, *Nat Commun 8*, 15861.

[3] Scobie, H. M., Rainey, G. J. A., Bradley, K. A., and Young, J. A. T. (2003) HµMan capillary morphogenesis protein 2 functions as an anthrax toxin receptor, *P Natl Acad Sci USA 100*, 5170-5174.

[4] Santelli, E., Bankston, L. A., Leppla, S. H., and Liddington, R. C. (2004) Crystal structure of a complex between anthrax toxin and its host cell receptor, *Nature 430*, 905-908.

[5] Liu, S., Crown, D., Miller-Randolph, S., Moayeri, M., Wang, H., Hu, H., Morley, T., and Leppla, S. H. (2009) Capillary morphogenesis protein-2 is the major receptor mediating lethality of anthrax toxin in vivo, *Proc Natl Acad Sci U S A 106*, 12424-12429.

[6] Lacy, D. B., Wigelsworth, D. J., Scobie, H. M., Young, J. A. T., and Collier, R. J. (2004) Crystal structure of the von Willebrand factor A domain of hµMan capillary morphogenesis protein 2: An anthrax toxin receptor, *P Natl Acad Sci USA 101*, 6367-6372.

[7] Scobie, H. M., Thomas, D., Marlett, J. M., Destito, G., Wigelsworth, D. J., Collier, R. J., Young, J. A., and Manchester, M. (2005) A soluble receptor decoy protects rats against anthrax lethal toxin challenge, *J Infect Dis 192*, 1047-1051.

[8] Rogers, M. S., Christensen, K. A., Birsner, A. E., Short, S. M., Wigelsworth, D. J., Collier, R. J., and D'Amato, R. J. (2007) Mutant anthrax toxin B moiety (protective antigen) inhibits angiogenesis and tµMor growth, *Cancer Res 67*, 9980-9985.

[9] Reeves, C. V., Dufraine, J., Young, J. A. T., and Kitajewski, J. (2010) Anthrax toxin receptor 2 is expressed in murine and tµMor vasculature and functions in endothelial proliferation and morphogenesis, *Oncogene 29*, 789-801.

[10] Cryan, L. M., Bazinet, L., Habeshian, K. A., Cao, S., Clardy, J., Christensen, K. A., and Rogers, M. S. (2013) 1,2,3,4,6-Penta-O-galloyl-beta-D-glucopyranose inhibits angiogenesis via inhibition of capillary morphogenesis gene 2, *J Med Chem 56*, 1940-1945.

[11] Cao, S., Cryan, L., Habeshian, K. A., Murillo, C., Tamayo-Castillo, G., Rogers, M. S., and Clardy, J. (2012) Phenolic compounds as antiangiogenic CMG2 inhibitors from Costa Rican endophytic fungi, *Bioorg Med Chem Lett 22*, 5885-5888.

[12] Cryan, L. M., and Rogers, M. S. (2011) Targeting the anthrax receptors, TEM-8 and CMG-2, for anti-angiogenic therapy, *Front Biosci (Landmark Ed) 16*, 1574-1588.

[13] Rogers, M. S., Cryan, L. M., Habeshian, K. A., Bazinet, L., Caldwell, T. P., Ackroyd, P. C., and Christensen, K. A. (2012) A FRET-Based High Throughput Screening Assay to Identify Inhibitors of Anthrax Protective Antigen Binding to Capillary Morphogenesis Gene 2 Protein, *Plos One 7*.

[14] El-Kamah, G. Y., Fong, K., El-Ruby, M., Affifi, H. H., Clements, S. E., Lai-Cheong, J. E., Amr, K., El-Darouti, M., and McGrath, J. A. (2010) SpectrµM of mutations in the ANTXR2 (CMG2) gene in infantile systemic hyalinosis and juvenile hyaline fibromatosis, *Brit J Dermatol 163*, 213-215.
[15] Dowling, O., Difeo, A., Ramirez, M. C., Tukel, T., Narla, G., Bonafe, L., Kayserili, H., Yuksel-Apak, M., Paller, A. S., Norton, K., Teebi, A. S., GrµM-Tokars, V., Martin, G. S., Davis, G. E., Glucksman, M. J., and Martignetti, J. A. (2003) Mutations in capillary morphogenesis gene-2 result in the allelic disorders juvenile hyaline fibromatosis and infantile systemic hyalinosis, *Am J HµM Genet 73*, 957-966.
[16] Deuquet, J., Lausch, E., Superti-Furga, A., and van der Goot, F. G. (2012) The dark sides of capillary morphogenesis gene 2, *Embo J 31*, 3-13.
[17] Hanks, S., Adams, S., Douglas, J., Arbour, L., Atherton, D. J., Balci, S., Bode, H., Campbell, M. E., Feingold, M., Keser, G., Kleijer, W., Mancini, G., McGrath, J. A., Muntoni, F., Nanda, A., Teare, M. D., Warman, M., Pope, F. M., Superti-Furga, A., Futreal, P. A., and Rahman, N. (2003) Mutations in the gene encoding capillary morphogenesis protein 2 cause juvenile hyaline fibromatosis and infantile systemic hyalinosis, *Am J HµM Genet 73*, 791-800.
[18] Kalluri, R. (2003) Basement membranes: Structure, assembly and role in tµMour angiogenesis, *Nature Reviews Cancer 3*, 422-433.
[19] Kamphaus, G. D., Colorado, P. C., Panka, D. J., Hopfer, H., Ramchandran, R., Torre, A., Maeshima, Y., Mier, J. W., Sukhatme, V. P., and Kalluri, R. (2000) Canstatin, a novel matrix-derived inhibitor of angiogenesis and tµMor growth, *J Biol Chem 275*, 1209-1215.
[20] Nyberg, P., Xie, L., Sugimoto, H., Colorado, P., Sund, M., Holthaus, K., Sudhakar, A., Salo, T., and Kalluri, R. (2008) Characterization of the anti-angiogenic properties of arresten, an alpha1beta1 integrin-dependent collagen-derived tµMor suppressor, *Exp Cell Res 314*, 3292-3305.
[21] Monboisse, J. C., Oudart, J. B., Ramont, L., Brassart-Pasco, S., and Maquart, F. X. (2014) Matrikines from basement membrane collagens: A new anti-cancer strategy, *Biochimica Et Biophysica Acta-General Subjects 1840*, 2589-2598.
[22] Panka, D. J., and Mier, J. W. (2003) Canstatin inhibits Akt activation and induces Fas-dependent apoptosis in endothelial cells, *J Biol Chem 278*, 37632-37636.
[23] Magnon, C., Galaup, A., Mullan, B., Rouffiac, V., Bouquet, C., Bidart, J. M., Griscelli, F., Opolon, P., and Perricaudet, M. (2005) Canstatin acts on endothelial and tµMor cells via mitochondrial damage initiated through interaction with alphavbeta3 and alphavbeta5 integrins, *Cancer Res 65*, 4353-4361.
[24] Sudhakar, A., Nyberg, P., Keshamouni, V. G., Mannam, A. P., Li, J., Sugimoto, H., Cosgrove, D., and Kalluri, R. (2005) HµMan alpha1 type IV collagen NC1 domain exhibits distinct antiangiogenic activity mediated by alpha1beta1 integrin, *J Clin Invest 115*, 2801-2810.
[25] Wigelsworth, D. J., Krantz, B. A., Christensen, K. A., Lacy, D. B., Juris, S. J., and Collier, R. J. (2004) Binding stoichiometry and kinetics of the interaction of a hµMan anthrax toxin receptor, CMG2, with protective antigen, *J Biol Chem 279*, 23349-23356.
[26] Schrodinger, LLC. (2015) The PyMOL Molecular Graphics System, Version 1.8.
[27] Andreatta, M., Lund, O., and Nielsen, M. (2013) Simultaneous alignment and clustering of peptide data using a Gibbs sampling approach, *Bioinformatics 29*, 8-14.
[28] Andreatta, M., Alvarez, B., and Nielsen, M. (2017) GibbsCluster: unsupervised clustering and alignment of peptide sequences, *Nucleic Acids Res*.

[29] Thomsen, M. C., and Nielsen, M. (2012) Seq2Logo: a method for construction and visualization of amino acid binding motifs and sequence profiles including sequence weighting, pseudo counts and two-sided representation of amino acid enrichment and depletion, *Nucleic Acids Res 40*, W281-287.
[30] Obeso, J., Weber, J., and Auerbach, R. (1990) A hemangioendothelioma-derived cell line: its use as a model for the study of endothelial cell biology, *Lab Invest 63*, 259-269.
[31] Ahn, K., Pan, S., Beningo, K., and Hupe, D. (1995) A permanent hµMan cell line (EA.hy926) preserves the characteristics of endothelin converting enzyme from primary hµMan µMbilical vein endothelial cells, *Life Sci 56*, 2331-2341.
[32] Than, M. E., Henrich, S., Huber, R., Ries, A., Mann, K., Kuhn, K., Timpl, R., Bourenkov, G. P., Bartunik, H. D., and Bode, W. (2002) The 1.9-A crystal structure of the noncollagenous (NC1) domain of hµMan placenta collagen IV shows stabilization via a novel type of covalent Met-Lys cross-link, *Proc Natl Acad Sci U S A 99*, 6607-6612.
[33] Plow, E. F., Haas, T. K., Zhang, L., Loftus, J., and Smith, J. W. (2000) Ligand binding to integrins, *J Biol Chem 275*, 21785-21788.
[34] Lacy, D. B., Wigelsworth, D. J., Melnyk, R. A., Harrison, S. C., and Collier, R. J. (2004) Structure of heptameric protective antigen bound to an anthrax toxin receptor: A role for receptor in pH-dependent pore formation, *P Natl Acad Sci USA 101*, 13147-13151.
[35] E, G. D., Carrero, P., Madrona, A., Rodriguez-Salamanca, P., Martinez-Gualda, B., Camarasa, M. J., Jimeno, M. L., Bennallack, P. R., Finnell, J. G., Tsang, T. M., Christensen, K. A., San-Felix, A., and Rogers, M. S. (2019) Galloyl Carbohydrates with Antiangiogenic Activity Mediated by Capillary Morphogenesis Gene 2 (CMG2) Protein Binding, *J Med Chem 62*, 3958-3970.
[36] Nanda, A., Carson-Walter, E. B., Seaman, S., Barber, T. D., Stampfl, J., Singh, S., Vogelstein, B., Kinzler, K. W., and St Croix, B. (2004) TEM8 interacts with the cleaved C5 domain of collagen alpha 3(VI), *Cancer Res 64*, 817-820.
[37] Werner, E., Kowalczyk, A. P., and Faundez, V. (2006) Anthrax toxin receptor 1/tµMor endotheliµM marker 8 mediates cell spreading by coupling extracellular ligands to the actin cytoskeleton, *J Biol Chem 281*, 23227-23236.
[38] Tomoda, H., Kishimoto, Y., and Lee, Y. C. (1989) Temperature effect on endocytosis and exocytosis by rabbit alveolar macrophages, *J Biol Chem 264*, 15445-15450.
[39] Abrami, L., Bischofberger, M., Kunz, B., Groux, R., and van der Goot, F. G. (2010) Endocytosis of the Anthrax Toxin Is Mediated by Clathrin, Actin and Unconventional Adaptors, *Plos Pathog 6*.
[40] Abrami, L., Liu, S. H., Cosson, P., Leppla, S. H., and van der Goot, F. G. (2003) Anthrax toxin triggers endocytosis of its receptor via a lipid raft-mediated clathrin-dependent process, *Journal of Cell Biology 160*, 321-328.
[41] Abrami, L., Leppla, S. H., and van der Goot, F. G. (2006) Receptor palmitoylation and ubiquitination regulate anthrax toxin endocytosis, *J Cell Biol 172*, 309-320.
[42] Abrami, L., Kunz, B., and van der Goot, F. G. (2010) Anthrax toxin triggers the activation of src-like kinases to mediate its own uptake, *P Natl Acad Sci USA 107*, 1420-1424.